Original Article

Mouse placental scaffolds: a three -dimensional environment model for recellularization

Journal of Tissue Engineering
Volume 10: 1–11

DOI: 10.1177/2041731419867962
journals.sagepub.com/home/tej
SAGE

Rodrigo SN Barreto[1*], Patricia Romagnolli[1,2*], Paula Fratini[1], Andrea Maria Mess[1] and Maria Angelica Miglino[1]

Abstract

The rich extracellular matrix (ECM) and availability make placenta eligible as alternative biomaterial source. Herein we produced placental mouse scaffolds by decellularization, and structure, composition, and cytocompatibility were evaluated to be considered as a biomaterial. We obtained a cell-free scaffold containing 9.42 ± 5.2 ng dsDNA per mg of ECM, presenting well-preserved structure and composition. Proteoglycans were widespread throughout ECM without cell nuclei and cell remnants. Collagen I, weak in native placenta, clearly appears in the scaffold after recellularization, opposite distribution was observed for collagen III. Fibronectin was well-observed in placental scaffolds whereas laminin and collagen IV were strong expressed. Placental scaffolds recellularization potential was confirmed after mouse embryonic fibroblasts 3D dynamic culture, resulting in massive scaffold repopulation with cell–cell interactions, cell-matrix adhesion, and maintenance of natural morphology. Our small size scaffolds provide a useful tool for tissue engineering to produce grafts and organ fragments, as well as for cellular biology purposes for tridimensional culture substrate.

Keywords

Tissue engineering, biomaterial, whole-placental scaffolds, extracellular matrix, recellularization

Received: 4 April 2019; accepted: 13 July 2019

Introduction

In tissue engineering, biomaterials and cells are used for tissue and/or organ regeneration,[1] by using a combination between engineering and biology approaches.[2] Biomaterials can be formed by three-dimensional (3D) biological microenvironments produced by decellularization, a tissue engineering technique to remove cells from organs, with minor disruption of their extracellular matrix (ECM) structure and composition.[3–5]

Usually biomaterials are produced by organ decellularization aiming to produce the same organ (or part of) by recellularization. However, organs availability is scarce, and searching for new biomaterial sources is needed. In this scenario, placenta that are usually discarded after birth without damage to the donors, and have a rich ECM could be an interesting alternative source to produce 3D scaffolds for further 3D culture recellularization, and produce small grafts.

The ECM from a decellularized tissue results in suitable scaffolds and is configured as a complex 3D structure, with functional protein and glycosaminoglycan composition.[6] Under this condition, bioactive ECM scaffolds are potential for cell repopulation and establishment of functional tissues.[4,7] Thus, scaffolds with minor DNA (<50 ng of dsDNA per mg of dry ECM)[5,8] are suitable for pre-clinical and clinical studies,[9] avoiding antigen gene expression and resulting in less immunological rejection after transplantation.[10]

Different techniques combining physical, chemical, and enzymatic agents are used for decellularization.[11] Detergents, such as sodium dodecyl sulfate (SDS) and octylphenol

[1]School of Veterinary Medicine and Animal Sciences, University of Sao Paulo, Sao Paulo, Brazil
[2]Federal University of the Southern Frontier, Realeza-PR, Brazil

*Shared first authorship

Corresponding author:
Maria Angelica Miglino, School of Veterinary Medicine and Animal Sciences, University of Sao Paulo, Av. Prof. Dr. Orlando Marques de Paiva, 87, University City "Armando Salles de Oliveira," Butantã, Sao Paulo 05508-270, Brazil.
Email: miglino@usp.br

ethoxylate (Triton X-100) are chemical agents commonly applied for decellularization[12] and can be combined with orbital agitation as mechanical agent supporter.[8]

SDS is an ionic detergent that efficiently lyse cells and solubilize cytoplasmic components, particularly in dense organs.[13] The expected effectiveness for SDS during decellularization seems related with the complexity of the organ in question, that is, 24 h of incubation at 0.1%–1% SDS concentrations[6]; or even at 0.01% as initial concentration.[14] However, SDS may compromise ECM structure and collagen integrity, when applied in high concentrations[4]; however, in low concentrations preserves better the ECM-related proteins.[15] By contrast, the mild non-ionic Triton X-100 action includes a moderate effect upon tissue architecture, resulting in minimal damage to the ECM structure.[6] Considered one of the best detergents to eliminate lipids from tissues,[8] Triton X-100 especially acts upon lipid–lipid and lipid–protein interactions.[16] Mild action of Triton X-100 allows its application in a broad range of time during decellularization, from 6 h to 14 days to improve cell removal, or less to remove residual SDS.[14]

A proper decellularization provides scaffolds that preserve ECM biocompatibility, biodegradability, and biomechanical resistance.[7,9] A glance over the ECM shows that its 3D structural organization and composition are related to multiple cellular functionalities.[17–19] Therefore, functional ECM on scaffolds are inductive materials for tissue and organ regeneration,[20] since recellularized with appropriate cells, including an optimal seeding method, and a physiologically relevant culture method.[21]

About culture methods on scaffolds, static and conventional two-dimensional (2D) culture recellularization are based on passive introduction of cell suspension into 3D scaffolds, with limited effectiveness by low seeding and minimal cell penetration.[3] However, 3D cell culture has been considered an excellent tool to mimic natural morphological and/or functional features of cells and tissues in vivo.[22] Herein, we will use a 3D dynamic culture, performed into a Rotary Cell Culture System (RCCS), that improved microgravity effect simulation, altering cells perception of gravitational direction, which is vital for cell movements[23,24] that could increases cell migration to inner areas of this small scaffold.

Materials and methods

Samples

This study was approved by Ethical Committee on Animal Use (Protocol ID.: 5669271015) of School of Veterinary Medicine and Animal Science of University of Sao Paulo, Sao Paulo, Brazil. In total, 112 mouse placentas (*Mus musculus*, C57BL/6) from day 18.5 of gestation were collected. Native placentas were weighed using an analytical balance (PA214CP, OHAUS) and measured in diameter using a Vernier caliper. Then placentas were washed three times with phosphate-buffered saline (PBS; 136.9 mM of NaCl, 26.8 mM of KCl, 14.7 mM of KH_2PO_4, and 8.1 mM of $Na_2HPO4.7H_2O$; pH 7.2) with 0.5% antibiotics (Penicillin-streptomycin, 15140130, Gibco), for 5 min each and used for the analysis.

Placental scaffolds production

Mouse placental decellularization lasted 5 days at room temperature under mechanical force induced by orbital agitation of 150 r/min (TS-2000A, VDRL Multifunctional Shaker, Biomixer). The first 3 days of decellularization protocol was conducted with SDS (13-1313-01, LGC Biotecnologia) diluted in distilled water at 0.01%, 0.1%, and 1% concentration, 1 day each, as proposed both to bovine and human placenta.[14] Subsequently, 1% Triton X-100 (13-1315-05, LGC Biotecnologia) in distilled water was applied for 2 days, in order to finalize cell content extraction and to remove the residual SDS. Finally, placental scaffolds were washed three times in PBS, for 15 min each and sterilized in ultraviolet light for 2 h. All applied solutions were supplement with 0.5% antibiotics.

Recellularization by 3D dynamic suspension cell culture

Mouse embryonic fibroblasts (SCRC-1049™, ATCC®) were thawed, centrifuged, and suspended in fibroblast proliferating medium (FPM) containing 88% Dulbecco's Modified Eagle Medium (DMEM, 12100046, Gibco), 10% fetal bovine serum (FBS, 10Bio500, LGC Biotecnologia), 1% non-essential amino acids (MEM NEAA, BR30238-01, LGC Biotecnologia), 1% amino acids (BME, B6766, Sigma), and 1 µL/mL antibiotics (Amikacin sulfate 16.68 µg/µL, Novafarma). Fibroblasts were placed on a culture flask, and cultured in an incubator, under humidified atmosphere of 5% CO_2 and at 37°C, until 80% confluence, then were resuspended to be reseeded on placental scaffolds in order to evaluate their potential for recellularization.

Recellularization was performed in 6 days, by dynamic suspension in a 3D RCCS (RCCS-4SC, Synthecon), under 13 r/min. First, 10 placental scaffolds were placed in a 10 mL sterile culture rotating wall vessel (RWV) bioreactor for 48 h, prior to recellularization, to stabilize the biomaterial in the culture environment contending FPM. Afterward, fibroblasts at density of 3 × 106 cells were added to the vessel containing placental scaffolds. Medium addition was performed with a syringe, while emptying bubble in the vessel with another syringe. Closing the sterile valves, vessel was mounted to the rotator base, and placed in 5% CO_2, 37°C incubator. Medium was changed every 24 h.

Histology

Native, decellularized, and recellularized 3D scaffolds were fixed in 4% paraformaldehyde (PFA) for 48 h and dehydrated in crescent concentrations of ethanol. Later on, samples were diaphanized in xylene, paraffin embedded, and sectioned (5 μm) in microtome (RM2265, Leica). Microsections were transferred to glass slides, and Hematoxylin-Eosin (HE, nuclei presence), Masson's Trichrome (connective tissue conformation), Colloidal Iron, and combined Alcian Blue-Periodic Acid-Schiff (PAB, glycosaminoglycans presence) stains were performed. The results were visualized using a light microscopy (Eclipse 80i, Nikon) and photographed using a digital camera (DS-Ri Color Digital Camera, Nikon).

Immunohistochemistry for paraffin-embedded tissues

To analyze ECM proteins in native and decellularized 3D scaffolds, sections (5 μm) of 4% PFA fixed and paraffin-embedded samples were transferred to poli-L-lysine (p8920, Sigma) coated glass slides. Then, tissues were treated with xylene, hydrated with decrescent ethanol concentrations, and rinsed with distilled water. Antigen retrieval was performed by heat-induced in citrate buffer (1.83 mM of monohydrate citric acid and 8.9 mM of sodium citrate tribasic dehydrate, pH 6.0). The endogenous peroxidase was blocked with 3% hydrogen peroxide in distilled water, at dark chamber and room temperature. Later on, nonspecific protein interaction was blocked with 2% bovine serum albumin (BSA) in tris-buffered saline (TBS; 2.0 mM of Trizma base and 1.36 mM of sodium chloride, pH 7.5) for 30 min at room temperature. Microsections were then incubated with the following primary antibodies: rabbit anti-collagen I (600-401-103S, 1:400, Rockland), goat anti-collagen III (sc-8779, 1:100, Santa Cruz Biotechnology), rabbit anti-collagen IV (1-CO083-0, 1:500, Quartett), rabbit anti-laminin subunit alpha-2 (bs-8561R, 1:200, Bioss Antibodies), and rabbit anti-fibronectin (NBP1-91258, 1:200, Novus Biologicals), overnight in a humidity chamber at 4°C. For negative controls, irrelevant anti-mouse IgG (M5284, Sigma) or anti-rabbit IgG (ab27478, Abcam) were used, in place of the primary antibodies. The reaction was detected with Dako Advance HRP kit (K6068, Dako, USA), developing the color with DAB + Substrate Chromogen System (K3468, Dako). A counter-staining was proceeded with hematoxylin. Washes with 0.2% BSA in TBS were performed at each step after primary antibody incubation. The slides were mounted and visualized using an Eclipse 80i microscope and photographed using a DS-Ri Color Digital Camera.

DAPI stain in frozen sections

Native and decellularized placentas were also analyzed for the presence of cellular nuclei by immunofluorescence. In both cases, samples were mounted in OCT embedding compound (4583-1, Sakura), frozen with liquid nitrogen vapor, and stored at –150°C. Tissue sections (40 μm) were produced using a cryostat (CM1520, Leica), thaw-mounted on to poli-L-lysine (p8920, Sigma) coated histological slides, and snap freeze at –150°C. Then, they were air dried and fixed in ice-cold acetone at –20°C. Thawing at room temperature, samples were washed with TBS. The coverslips were mounted with Prolong™ Gold Antifade Mountant with 4′,6-diamidino-2-phenylindole (DAPI) (P36931, Invitrogen), and visualized using a confocal microscope (FV1000, Olympus).

Whole-mounting immunofluorescence

Whole-placental 3D scaffolds recellularized with fibroblasts were fixed in 4% PFA and washed with PBS. Once air dried, the samples were washed with TBS and incubated with primary antibodies diluted in 0.2% BSA in TBS, in a humidified chamber at room temperature. The following primary antibodies were used: mouse anti-β2 tubulin (sc-47751, 1:100, Santa Cruz Biotechnology) and rabbit anti-collagen IV (ab6586, Abcam) for 1 h. Newly washed with TBS, tissues were incubated for another hour with secondary antibodies goat anti-mouse FITC (ab150113, Abcam) and goat anti-rabbit Alexa Fluor 568 (A-11011, Invitrogen), at 1:500 dilution in 0.2% BSA in TBS. After another wash with TBS, nuclear stain was provided applying Pierce DAPI Nuclear Counterstains (62248, 1:10.000, Thermo Scientific). The results were collected in a series of optical sections using confocal microscope (FV1000, Olympus).

Scanning electron microscopy

Native, decellularized, and recellularized placental samples were pre-fixed in 4% PFA for 48 h, and post-fixed in 1% osmium tetroxide for 90 min. Then, they were dehydrated in crescent concentrations of ethanol and dried using a critical point (EM CPD300, Leica). Later on, the samples were transferred and fixed on stubs and gold metalized (EMITECH K550). Visualizations were obtained using a scanning electron microscope (LEO 435VP SEM, LEO Electron Microscopy Ltd.).

Reminiscent genomic DNA quantification

Decellularized placentas were prepared as described by Barreto et al.,[25] and the genomic DNA quantification was performed with a Quant-iT™ DNA PicoGreen® dsDNA

Reagent (P7581, Invitrogen), according to the manufacturer's instructions. The final products were analyzed by spectrophotometry, measuring the absorbance at 530 nm in a microplate reader (μQuantTM, BioTek).

Results

We decellularized mouse placentas at E18.5 employing crescent concentrations of SDS (0.01%, 0.1%, and 1%), and 1% Triton X-100. Using this technique, we produced a cell-free placental ECM scaffolds, with well-preserved structure and composition. After decellularization, mouse placenta (Figure 1(a)) lost about 51.97% (±2.27) in weight and 54.26% (±6.06) in diameter, resulting on scaffolds with a mean diameter of 0.43 (±0.05) centimeters (Figure 1(b)). Compared to the native condition (Figure 1(c) and (e)), mouse placental scaffolds were absenting of cell nuclei when stained by HE (Figure 1(d)) and DAPI (Figure 1(f)) and persisted only 9.42 ± 5.2 ng dsDNA per mg of dry ECM an reduction of 85.9% in dsDNA. After decellularization, placental regions lost their natural appearance, remaining certain characteristics in its ECM spatial configuration, that is, former fetal vessels structure, which were helpful to estimate labyrinthine region (Figure 1(d)).

The Masson's Trichrome stain evidenced a native placental extracellular tissue permeated by their cellular populations (Figure 2(a)). By contrast, after decellularization, only the well-structured ECM was present (Figure 2(b)). The complex ultrastructural organization in native placental tissues were captured by SEM (Figure 2(c)). In decellularized placenta, the intricacy of fibrillar ECM proteins was observed in different arrangements among placental regions. In the junctional zone, delicate fibrils were interspersed by former vessel structures (Figure 2(d)), while labyrinthine fibrils were thicker and resembles a honeycomb structure due to fibrils mesh and spots in-between them (Figure 2(b) and (d)). Regarding general components, they were mostly similar among their distinct regions, both in native and decellularized mouse placental ECM. The proteoglycans distribution was accessed by PAB (Figure 2(e) and (f)) and Colloidal Iron stains (Figure 2(g) and (h)). Thereby, proteoglycans (blue stained) were widespread throughout labyrinth, junctional zone and decidua, both in native (Figure 2(e) and (f)) and decellularized placental ECM, however with less intensity in the later one (Figure 2(g) and (h)).

By immunohistochemistry, differences in intensity and localization of analyzed protein were evident, when comparing native and decellularized placenta (Figure 3). The collagen I in the stroma of native placenta at E18.5 was low present both in labyrinth and junctional zone, and absent in the decidua (Figure 3(a) and (b)). However, the scattered presence of collagen I in the ECM was better visualized in decellularized placenta in all regions (Figure 3(c)). Collagen III was largely detected in a strong

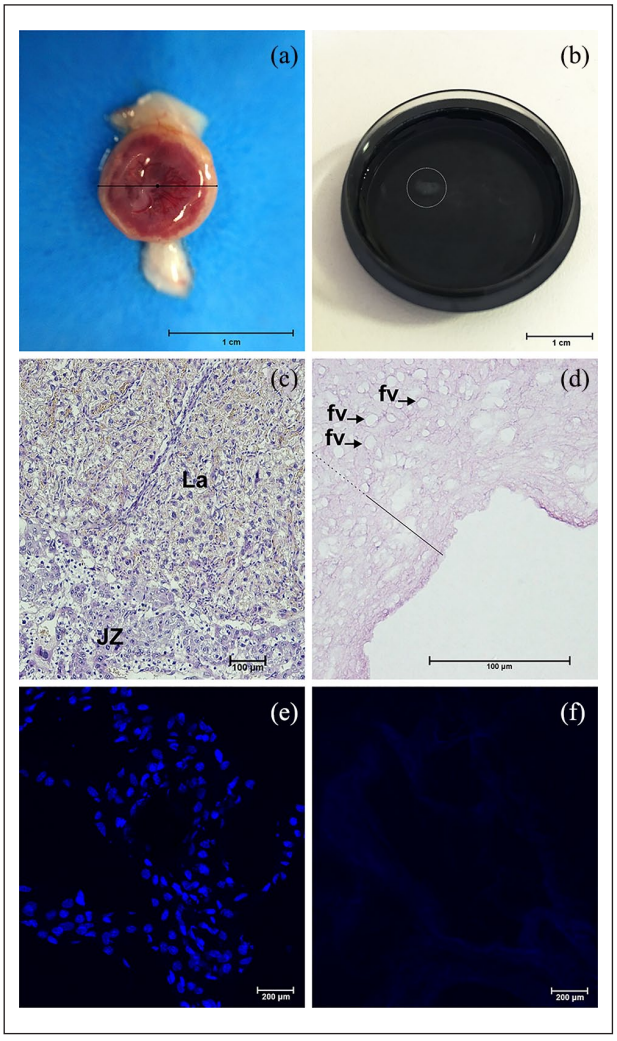

Figure 1. Decellularization of whole mouse placentas. Mouse placentas before (a) and after (b) decellularization process. Small scaffold floating in PBS on a 35 mm Petri dish (b). In Hematoxylin-Eosin stained tissue cell nuclei and other contents are normally visualized in native placental regions (c), but absent on the acellular ECM (d). In the decellularized ECM spatial configuration, placental regions were estimated considering the labyrinth (fill line) extension containing former fetal vessels structure (fv, arrows) and its continuous relationship with junctional zone and decidua (dashed line), respectively. The contrast between the nuclei presence (blue points stained) and absence were also noted in DAPI stains of native (e) and decellularized (f) placental tissues. JZ: junctional zone; La: labyrinth.
Scale bars = 1 cm (a, b), 100 μm (c, d), 200 μm (e, f).

presence within labyrinth and decidua, when compared to junctional zone (Figure 3(d) and (e)). Unexpectedly, collagen III was almost absent in the decellularized placenta (Figure 3(f)).

Data concerning the basement membrane showed that collagen IV had a strong presence in labyrinth, intermediate in junctional zone, and weak in decidua (Figure 3(g) and (h)). Similar intensities for collagen IV were detected

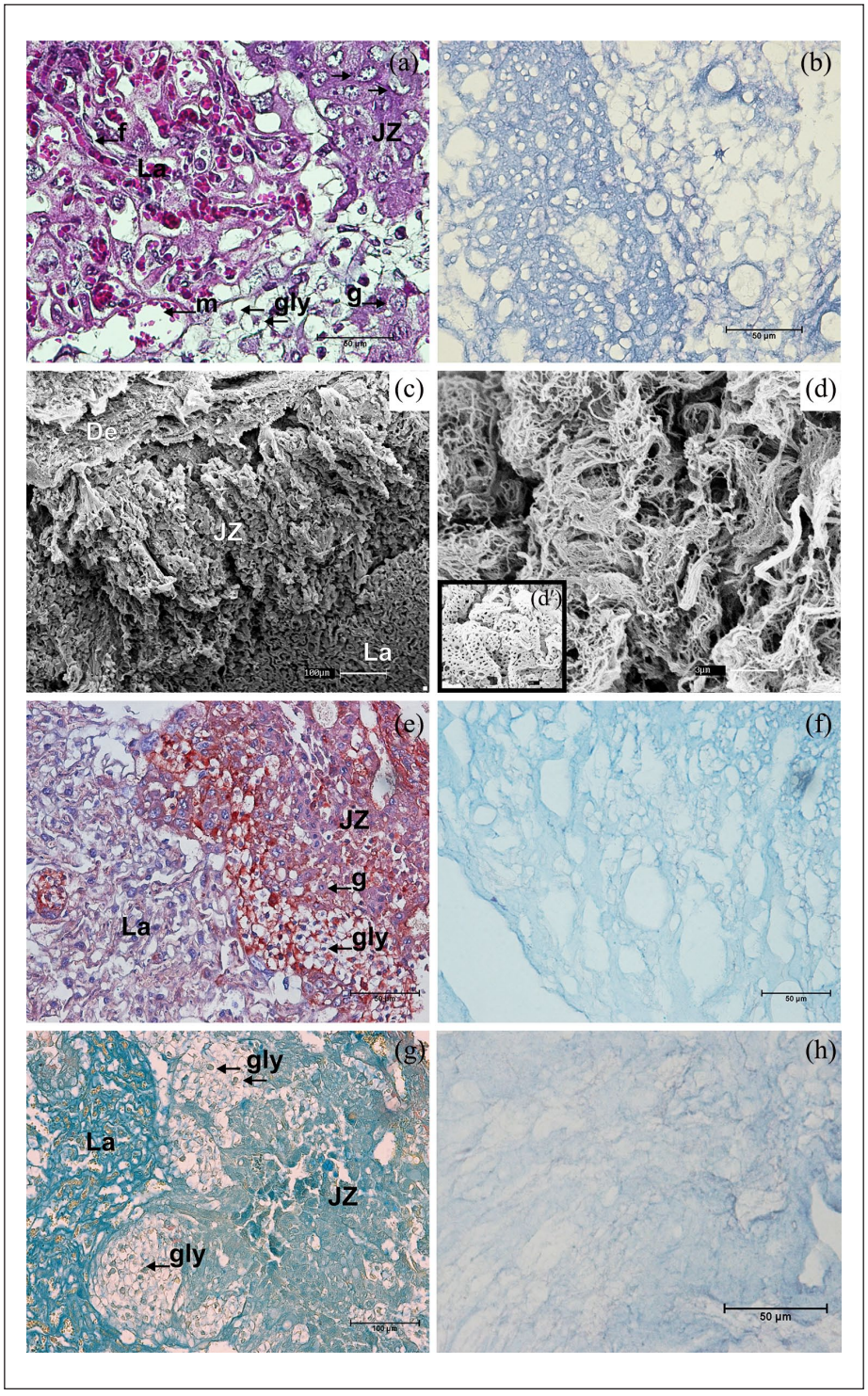

Figure 2. Structural analysis of mouse placenta. In the Masson's Trichrome stain (a), (b) a new spatial configuration is presented by an abundant and well-shaped decellularized placental ECM (b), after removal of usual cellular components (a). Ultrastructural analysis of mouse placenta by SEM (c), (d), (d'). The complex arrangement of the native placental regions (c) is also observed through cellular gaps on the scaffolds (d, d'). In-between the meshwork fibrils in the junctional zone, the angioarchitecture pattern was preserved (d), while a fibrillar honeycomb-like structural arrangement was observed in the labyrinth (d'). Proteoglycans were blue-colored in mouse placental ECM native placenta by combined Alcian Blue-PAS (e) and Colloidal Iron (g) stains, and similarly maintained decellularization (f), (h). De: decidua; JZ: junctional zone; La: labyrinth; f: fetal capillary; g: trophoblast giant cell; gly: trophoblast glycogen cell; m: maternal blood space.
Scale bars = 1 µm (d'), 3 µm (d), 50 µm (a, b, e, f, h), 100 µm (c, g).

in decellularized placenta, mainly surrounding their former vessels (Figure 3(i)). Laminin was observed at an intermediate level in labyrinth, being almost absent in junctional zone and weak in decidua (Figure 3(j) and (k)). In decellularized placenta, laminin was spread in intermediate level through the labyrinth (Figure 3(l)). Fibronectin was detected at intermediate levels within labyrinth of native (Figure 3(m) and (n)) and decellularized (Figure 3(o)) placenta. In native, fibronectin was not present in junctional zone and decidua (Figure 3(m) and (n)).

When testing the bioactivity properties of placental scaffolds for recellularization, fibroblasts 3D culture resulted in a repopulation of placental scaffolds. HE stains showed fibroblasts attached to the scaffold surface since day 3 (Figure 4(a) and (b)). At day 6, cells in the scaffold inner spaces was evident, also the 3D structure was better covered by the fibroblast, suggesting cell proliferation and migration (Figure 4(c)). The 3D placental scaffolds provided a microenvironment in which reseeded fibroblasts developed both cell-to-cell interactions (Figure 4(d)), and cell-matrix adhesions (Figure 4(e)). Besides, fibroblasts attached to placental ECM scaffolds preserved their rounded morphology (Figure 4(d) and (e)) in consequence of suspension culture, when compared to fibroblasts 2D cultured (Figure 4(f)). Even present in decellularized placental ECM the collagen IV apparently is remodeled by new cells (Figure 5(a) and (e)) due to alteration of their former distribution pattern (Figure 5(b) and (f). Spatial organization and integration adopted during fibroblasts migration and occupation of the new 3D microenvironment were pivotal for repopulation inner structures of the placental scaffolds (Figure 5(c), (d), (g), and (h)).

Discussion

Our results showed a biological scaffold derived from a small size whole organ decellularization. The new approach of using mouse placentas in tissue engineering was designed including the most common detergents employed for removing cells from tissues and organs,[4,12] in association with orbital agitation.[3] SDS concentrations and time of exposure, as previously established for human and cow placentomes,[14] were also favorable for mouse placentas decellularization. Finalized with Triton X-100 treatment,[4] decellularization resulted in well-preserved ECM within scaffolds. In association, both SDS and Triton X-100 provided less immunogenic scaffolds for further engraftments.[26] The weight and diameter losses in mouse placental scaffolds were the primary positive signs of cell removal.[27] The result also included the absence of cell nuclei as showed by histological analysis, in addition to low amount of reminiscent DNA as stated to a biological scaffold.[5,8] The structure of decellularized placental scaffolds revealed an acellular condition with minimal damage to the ECM,[28] as also stated.[29]

Apart from fibrillar protein that gives the ECM structure, proteoglycans and glycosaminoglycans fill ECM spaces, closely interacting with collagen fibrils, and acting as reservoir of several molecules, that is, growth factors, enzymes, and hormones.[30–32] Thus, the Colloidal Iron and PAB stains evidenced that the proteoglycans were maintained on the scaffolds after decellularization, at similar levels and distribution as in native placentas.

On the scaffolds, collagen I was almost absent, contrasting with those observed in the native placentas. Otherwise, collagen I could be detected in those regions of decellularized placenta where it was absent in native tissue. The interstitial collagens I and III fibrils are associated in soft tissues, both expressed in mouse and human placentas,[33,34] where the collagen I fibrils are structural components, and collagen III are related to the assembly and thickness of the fibrils.[35] In human placentas, the presence of collagen I fibrils are masked by the encasement of the collagen III,[36] being only exposed when collagen III is removed, that is, by 8 M urea in dermis,[37] or maybe by SDS in our model. Therefore, during decellularization, SDS may have modified and disrupted structurally the collagen III fibrils,[12] thus justifying their absence on the scaffolds, while it gave to the collagen I a better exposition. Alterations of this co-expression may change the mechanical properties of the fibrils.[38]

For collagen IV, its presence was overspread in all native placental regions, as predicted for mouse placentas.[39,40] Abundant in all of basement membranes, the maintenance of collagen IV on the placental scaffolds is a suitable characteristic for structural support to cell adhesion and migration.[17] Besides, the absence of collagen IV is correlated to the rupture of native ECM structure,[41,42] and its presence on placental scaffolds indicates structural integrity and functionality, thus favoring cell attachments.

Detected in native mouse placentas, fibronectin attaches the interstitial collagen system to the basement membranes.[36,39,43] Persisting to decellularization, fibronectin may facilitate adhesion to multiple cell types, making the scaffolds suitable for tissue culture.[44]

The laminin had similar distribution as collagen IV. This protein is localized on the lamina lucida of the basement membrane, situated in-between basal cell membrane and the lamina.[36,39,40,43] Also, it is an important element related to the organization and maintenance of vascular structures.[44]

Fibronectin, collagen IV, and laminin are the main ECM basement membrane components,[41] and their maintenance after decellularization is an important indicative of scaffolds bioactivity for future applications.

The 3D environment installed on placental scaffolds effectively supported cells, allowing cell repopulation,[45] cell proliferation, and migration.[46] Surpassing the traditional and static 2D culture, the 3D culture environment can be further increased by dynamic mechanisms to reseed

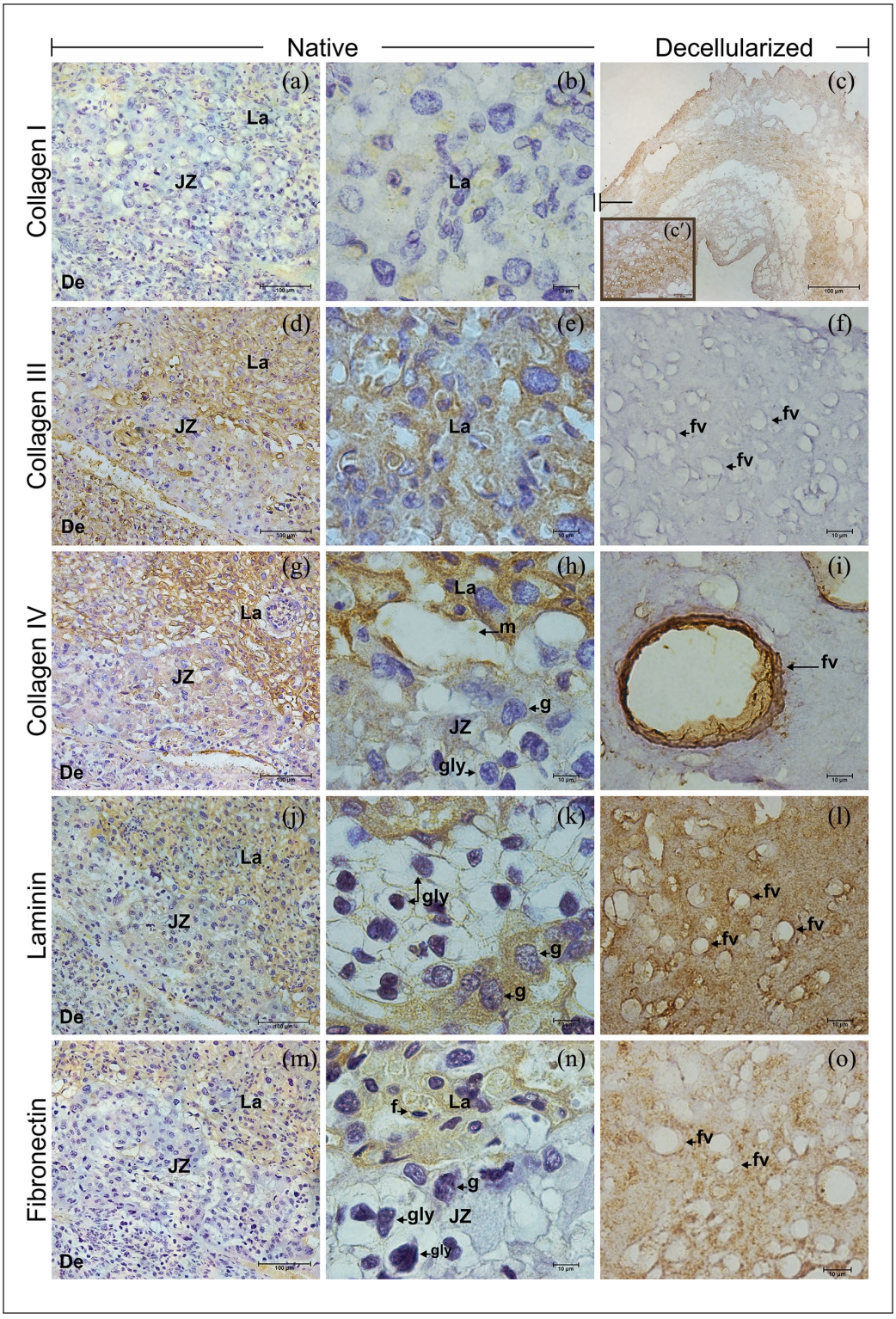

Figure 3. Immunohistochemistry for collagens I, III, and IV, laminin and fibronectin in native and decellularized mouse placenta. Collagen I was lightly visualized in native (a), (b) and unexpectedly strong spread in the ECM after decellularization (c), (c′). Unlike, the collagen III observed in native (d), (e), was absent in the scaffolds (f). Collagen IV (g), (h), laminin (j), (k), and fibronectin (m), (n) had similar distribution in the native placental regions, except by the fibronectin absence in the junctional zone (n). In the acellular ECM, the mainly collagen IV (i), but also laminin (l) and fibronectin (o) surrounded the former fetal vessels. De: decidua; JZ: junctional zone; La: labyrinth; f: fetal capillary; fv: former fetal vessel; g: trophoblast giant cell; gly: trophoblast glycogen cell; m: maternal blood space. Scale bars = 100 µm (a, c, d, g, j, m), 50 µm (c′), 10 µm (b, e, f, h, i, k, l, n, o).

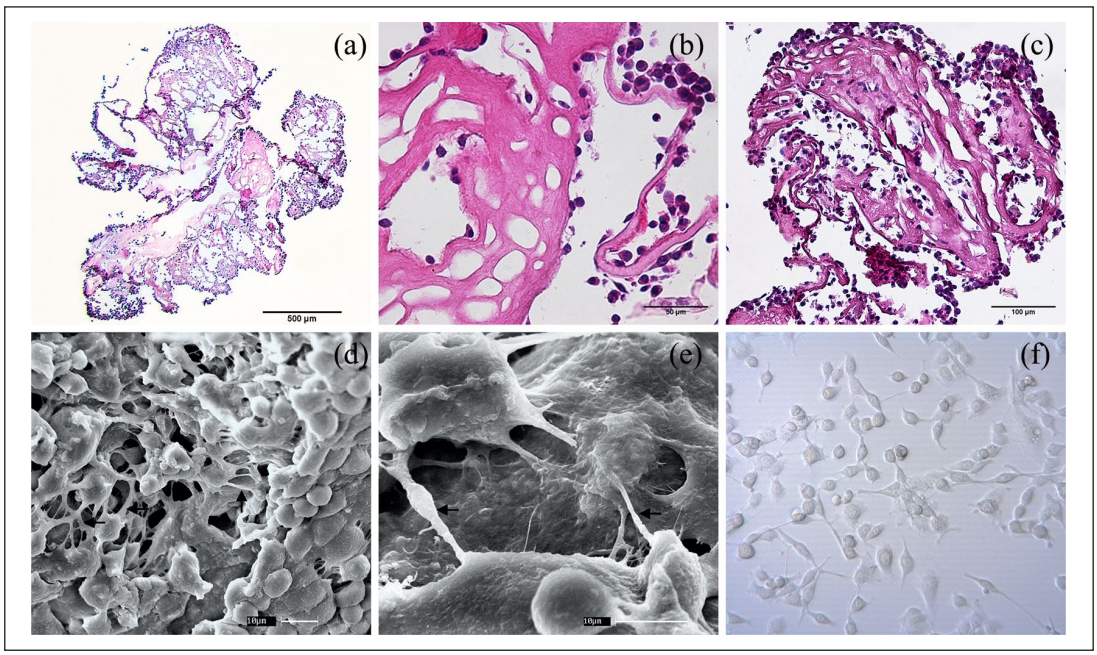

Figure 4. Placental scaffolds recellularized with mouse embryonic fibroblasts in a dynamic 3D culture system. Hematoxylin-Eosin stained placental scaffold after 3 (a), (b) and 6 (c) days of recellularization. Initially, fibroblasts adhered to the outer surface of the scaffold (a, b), later migrating through the extracellular matrix to internal regions (c). Scanning electron microscopy analysis of three-dimensional fibroblast growth on placental scaffold under 6 days of dynamic culture (e), (f). Fibroblasts distributed throughout the placenta scaffold interacting with each other (d), and adhering to the extracellular matrix by their cytoplasmic extensions (e, arrows). Round-shaped cells where obtained by 3D suspension dynamic culture (d), (e), comparing with the flattened fibroblast cultured in 2D static culture (f).
Scale bars = 500 μm (a), 100 μm (c), 50 μm (b), 30 μm (d), 10 μm (d, e), 1 μm (d).

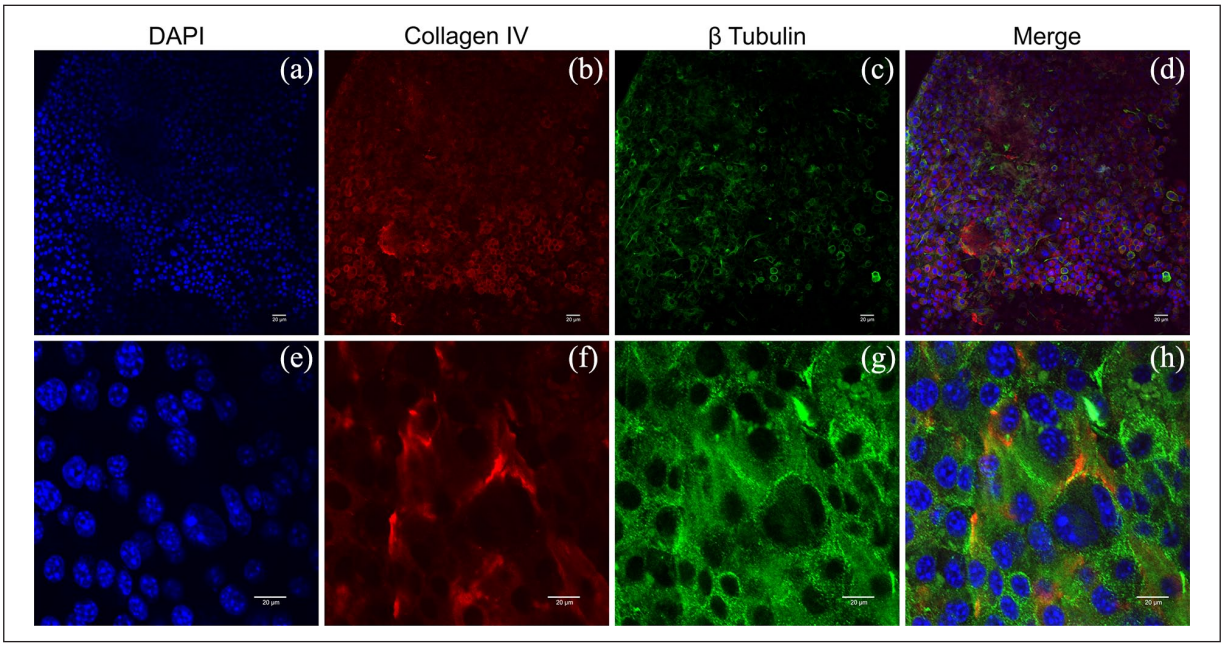

Figure 5. Whole-mount immunofluorescence on mouse placental scaffolds recellularized with mouse embryonic fibroblasts, using collagen IV (b), (f), and β tubulin (c), (g) antibodies. With a high cellular concentration, collagen IV present in placental scaffold is remodeled (b), (f), during the reorganization of the fibroblasts on the scaffold surface. Cytoplasmic microtubules evolved in fibroblasts motility mechanism are characteristically expressing β Tubulin (c), (g). Nuclei were stained with DAPI (a), (e), and merge images produced for full view (d), (h).
Scale bars = 20 μm.

cell population.[3,47] Indeed, using the RCCS, the embryonic mouse fibroblasts reseeded on placental scaffolds by 3D dynamic cell culture promoted placental tissue recellularization such as in lung scaffolds, promoting both cell growth and differentiation.[48] The natural morphology preserved by mouse embryonic fibroblasts attached to ECM scaffolds is another benefit of RCCS. Natural cellular morphology is an expected characteristic when mechanical cellular damage is reduced by maintaining a low shearing force, within the fluid during rotating culture, and also avoiding bubbles due to turbulence caused by the rotary motion.[47]

Once established, the production of small size whole-placental scaffolds may contribute in studies upon cell-to-cell and cell-to-ECM interactions,[2,49,50] providing a biological 3D microenvironment for cell culture.[51] It can be advantageous to observe placental scaffolds as a promise source of 3D microenvironment ready to be used in Regenerative Medicine routine, that is, human placenta and cow placentome scaffolds as auxiliary liver connections to the systemic circulation,[14] and as support to hepatic tissue in acute liver failure.[52] In fact, cow placentomes are considered as interesting alternatives to develop large-scale scaffolds with complex vascular architecture.[25] A small whole-placental scaffold may improve the mouse placenta model,[53] placing an acellular 3D microenvironment in the panel of trophoblast studies, overcoming the traditional monolayers.[54] Trophoblast were also seen as a model of primary syncytiotrophoblast, based on 3D dynamic culture.[22] However, by unifying 3D placental environments with dynamic 3D culture assays, a new model in trophoblast research can raise. A model in which trophoblasts could be seeded, cultured, and studied on their natural environment, or even had their development accompanied since their cellular precursors, that is, murine fibroblasts.[55]

In conclusion, placental scaffolds can be produced by decellularization with preserved ECM structure and composition, and it can be recellularized, serving as a 3D environment for tissue engineering and cellular biology purposes.

Acknowledgements

We warmly thank Anthony Carter from University of Southern Denmark for fruitful discussions. We are very grateful to Karl Klisch from University of Zürich for providing ECM antibodies. We thank Rose E. G. Rici from Advanced Center of Image Diagnosis of University of Sao Paulo for microscopy analysis supporting.

Declaration of conflicting interests

The author(s) declared no potential conflicts of interest with respect to the research, authorship, and/or publication of this article.

Funding

The author(s) disclosed receipt of the following financial support for the research, authorship, and/or publication of this article: The authors have received grants from Sao Paulo Research Foundation (14/50844-3) and from National Council for Scientific and Technological Development (467476/2014-4).

ORCID iDs

Rodrigo SN Barreto https://orcid.org/0000-0001-5240-6959
Maria Angelica Miglino https://orcid.org/0000-0003-4979-115X

References

1. Katari R, Peloso A and Orlando G. Tissue engineering and regenerative medicine: semantic considerations for an evolving paradigm. *Front Bioeng Biotechnol* 2015; 2: 57.
2. Keane TJ and Badylak SF. Biomaterials for tissue engineering applications. *Semin Pediat Surg* 2014; 23: 112–118.
3. Fu RH, Wang YC, Liu SP, et al. Decellularization and recellularization technologies in tissue engineering. *Cell Transplant* 2014; 23(4–5): 621–630.
4. Keane TJ, Swinehart IT and Badylak SF. Methods of tissue decellularization used for preparation of biologic scaffolds and in vivo relevance. *Methods* 2015; 84: 25–34.
5. Syed O, Walters NJ, Day RM, et al. Evaluation of decellularization protocols for production of tubular small intestine submucosa scaffolds for use in oesophageal tissue engineering. *Acta Biomater* 2014; 10(12): 5043–5054.
6. Hrebikova H, Diaz D and Mokry J. Chemical decellularization: a promising approach for preparation of extracellular matrix. *Biomed Pap Med Fac Univ Palacky Olomouc Czech Repub* 2015; 159(1): 12–17.
7. de Kemp V, de Graaf P, Fledderus JO, et al. Tissue engineering for human urethral reconstruction: systematic review of recent literature. *PLoS ONE* 2015; 10(2): e0118653.
8. Crapo PM, Gilbert TW and Badylak SF. An overview of tissue and whole organ decellularization processes. *Biomaterials* 2011; 32(12): 3233–3243.
9. Xu Y, Xu GY, Tang C, et al. Preparation and characterization of bone marrow mesenchymal stem cell-derived extracellular matrix scaffolds. *J Biomed Mater Res B Appl Biomater* 2015; 103(3): 670–678.
10. Methe K, Backdahl H, Johansson BR, et al. An alternative approach to decellularize whole porcine heart. *Biores Open Access* 2014; 3(6): 327–338.
11. Gilbert TW, Sellaro TL and Badylak SF. Decellularization of tissues and organs. *Biomaterials* 2006; 27(19): 3675–3683.
12. Faulk DM, Carruthers CA, Warner HJ, et al. The effect of detergents on the basement membrane complex of a biologic scaffold material. *Acta Biomater* 2014; 10(1): 183–193.
13. Uygun BE, Soto-Gutierrez A, Yagi H, et al. Organ reengineering through development of a transplantable recellularized liver graft using decellularized liver matrix. *Nat Med* 2010; 16: 814–820.
14. Kakabadze A and Kakabadze Z. Prospect of using decellularized human placenta and cow placentome for creation

of new organs: targeting the liver (part I: anatomic study). *Transplant Proc* 2015; 47(4): 1222–1227.
15. Gilpin SE, Guyette JP, Gonzalez G, et al. Perfusion decellularization of human and porcine lungs: Bringing the matrix to clinical scale. *J Heart Lung Transplant* 2014; 33(3): 298–308.
16. Yam GHF, Yusoff NZBM, Goh TW, et al. Decellularization of human stromal refractive lenticules for corneal tissue engineering. *Sci Rep* 2016; 6: 26339.
17. Oefner CM, Sharkey A, Gardner L, et al. Collagen type IV at the fetal-maternal interface. *Placenta* 2015; 36(1): 59–68.
18. Park YB, Seo S, Kim JA, et al. Effect of chondrocyte-derived early extracellular matrix on chondrogenesis of placenta-derived mesenchymal stem cells. *Biomed Mater* 2015; 10(3): 035014.
19. Xing Q, Yates K, Tahtinen M, et al. Decellularization of fibroblast cell sheets for natural extracellular matrix scaffold preparation. *Tissue Eng Part C Methods* 2015; 21(1): 77–87.
20. Pan J, Yan S, Gao JJ, et al. In-vivo organ engineering: Perfusion of hepatocytes in a single liver lobe scaffold of living rats. *Int J Biochem Cell Biol* 2016; 80: 124–131.
21. Scarritt ME, Pashos NC and Bunnell BA. A review of cellularization strategies for tissue engineering of whole organs. *Front Bioeng Biotechnol* 2015; 3: 43–17.
22. McConkey CA, Delorme-Axford E, Nickerson CA, et al. A three-dimensional culture system recapitulates placental syncytiotrophoblast development and microbial resistance. *Sci Adv* 2016; 2(3): e1501462.
23. Tang Y, Xu Y, Xiao Z, et al. The combination of three-dimensional and rotary cell culture system promotes the proliferation and maintains the differentiation potential of rat BMSCs. *Sci Rep* 2017; 7(1): 192–115.
24. Wolf DA and Kleis SJ. Principles of analogue and true microgravity bioreactors to tissue engineering. In: Nickerson CA, Pellis NR and Ott CM (eds) *Effect of spaceflight and spaceflight analogue culture on human and microbial cells*. New York: Springer, 2016, pp.39–60.
25. Barreto RSN, Romagnolli P, Mess AM, et al. Decellularized bovine cotyledons may serve as biological scaffolds with preserved vascular arrangement. *J Tissue Eng Regen Med* 2018; 12(4): e1880–e1888.
26. Price AP, Godin LM, Domek A, et al. Automated decellularization of intact, human-sized lungs for tissue engineering. *Tissue Eng Part C Methods* 2015; 21(1): 94–103.
27. Oliveira AC, Garzon I, Ionescu AM, et al. Evaluation of small intestine grafts decellularization methods for corneal tissue engineering. *PLoS ONE* 2013; 8(6): e66538.
28. Badylak SF, Freytes DO and Gilbert TW. Extracellular matrix as a biological scaffold material: Structure and function. *Acta Biomaterialia* 2009; 5: 1–13.
29. Pati F, Jang J, Ha D-H, et al. Printing three-dimensional tissue analogues with decellularized extracellular matrix bioink. *Nat Commun* 2014; 5: 3935.
30. Junqueira LC and Montes GS. Biology of collagen-proteoglycan interaction. *Arch Histol Jpn* 1983; 46(5): 589–629.
31. Scott JE. Proteoglycan-collagen interactions. *Ciba Found Symp* 1986; 124: 104–124.
32. Wu Z, Tang Y, Fang H, et al. Decellularized scaffolds containing hyaluronic acid and EGF for promoting the recovery of skin wounds. *J Mater Sci Mater Med* 2015; 26(1): 5322.
33. Cameron GJ, Alberts IL, Laing JH, et al. Structure of type I and type III heterotypic collagen fibrils: an X-Ray diffraction study. *J Struct Biol* 2002; 137(1–2): 15–22.
34. Malak TM, Ockleford CD, Bell SC, et al. Confocal immunofluorescence localization of collagen types I, III, IV, V and VI and their ultrastructural organization in term human fetal membranes. *Placenta* 1993; 14(4): 385–406.
35. Spiess K and Zorn TM. Collagen Types I, III, and V constitute the thick collagen fibrils of the mouse decidua. *Microsc Res Tech* 2007; 70(1): 18–25.
36. Amenta PS, Gay S, Vaheri A, et al. The extracellular matrix is an integrated unit: ultrastructural localization of collagen types I, III, IV, V, VI, fibronectin, and laminin in human term placenta. *Coll Relat Res* 1986; 6(2): 125–152.
37. Fleischmajer R, MacDonald DE, Perlish JS, et al. Dermal collagen fibrils of type I and type III collagen molecules. *J Struct Biol* 1990; 105: 162–169.
38. Asgari M, Latifi N, Heris HK, et al. In vitro fibrillogenesis of tropocollagen type III in collagen type I affects its relative fibrillar topology and mechanics. *Sci Rep* 2017; 7(1): 1392.
39. Saylam C, Ozdemir N, Itil IM, et al. Distribution of fibronectin, laminin and collagen type IV in the materno-fetal boundary zone of the developing mouse placenta. *Arch Gynecol Obstet* 2002; 266(2): 83–85.
40. Thomas T and Dziadek M. Differential expression of laminin, nidogen and collagen IV genes in the midgestation mouse placenta. *Placenta* 1993; 14(6): 701–713.
41. Poschl E, Schlotzer-Schrehardt U, Brachvogel B, et al. Collagen IV is essential for basement membrane stability but dispensable for initiation of its assembly during early development. *Development* 2004; 131(7): 1619–1628.
42. Schenke-Layland K, Angelis E, Rhodes KE, et al. Collagen IV induces trophoectoderm differentiation of mouse embryonic stem cells. *Stem Cells* 2007; 25(6): 1529–1538.
43. Giachini FRC, Carriel V, Capelo LP, et al. Maternal diabetes affects specific extracellular matrix components during placentation. *J Anat* 2008; 212(1): 31–41.
44. Londono R and Badylak SF. Biologic scaffolds for regenerative medicine: mechanisms of in vivo remodeling. *Ann Biomed Eng* 2015; 43(3): 577–592.
45. Gilpin SE, Ren X, Okamoto T, et al. Enhanced lung epithelial specification of human induced pluripotent stem cells on decellularized lung matrix. *Ann Thorac Surg* 2014; 98(5): 1721–1729.
46. Willemse J, Lieshout R, Van Der Laan LJW, et al. From organoids to organs: bioengineering liver grafts from hepatic stem cells and matrix. *Best Pract Res Clin Gastroenterol* 2017; 31(2): 151–159.
47. Pao SI, Chien KH, Lin HT, et al. Effect of microgravity on the mesenchymal stem cell characteristics of limbal fibroblasts. *J Chin Med Assoc* 2017; 80(9): 595–607.
48. Crabbe A, Liu Y, Sarker SF, et al. Recellularization of decellularized lung scaffolds is enhanced by dynamic suspension culture. *PLoS ONE* 2015; 10(5): e0126846.
49. Franczyk M, Lopucki M, Stachowicz N, et al. Extracellular matrix proteins in healthy and retained placentas, comparing

hemochorial and synepitheliochorial placentas. *Placenta* 2017; 50: 19–24.
50. Schneider KH, Aigner P, Holnthoner W, et al. Decellularized human placenta chorion matrix as a favorable source of small-diameter vascular grafts. *Acta Biomater* 2016; 29: 125–134.
51. Robins JC, Morgan JR, Krueger P, et al. Bioengineering anembryonic human trophoblast vesicles. *Reprod Sci* 2011; 18(2): 128–135.
52. Kakabadze Z, Kakabadze A, Chakhunashvili D, et al. Decellularized human placenta supports hepatic tissue and allows rescue in acute liver failure. *Hepatology* 2018; 67(5): 1956–1969.
53. Carter AM. Animal models of human placentation: a review. *Placenta* 2007; 28(Suppl. A): S41–S47.
54. Rai A and Cross JC. Three-dimensional cultures of trophoblast stem cells autonomously develop vascular-like spaces lined by trophoblast giant cells. *Dev Biol* 2015; 398(1): 110–119.
55. Kubaczka C, Senner CE, Cierlitza M, et al. Direct induction of trophoblast stem cells from murine fibroblasts. *Cell Stem Cell* 2015; 17(5): 557–568.